Mon. Not. R. Astron. Soc. **000**, 1–9 (2002) Printed 16 January 2014 (MN LATEX style file v2.2)

MOCCA code for star cluster simulations – III. Stellar-mass black holes in the globular cluster M22

Douglas C. Heggie[1⋆] and Mirek Giersz[2]
[1]*School of Mathematics and Maxwell Institute for Mathematical Sciences, University of Edinburgh, King's Buildings, Edinburgh EH9 3JZ, UK*
[2]*Nicolaus Copernicus Astronomical Centre, Polish Academy of Sciences, ul. Bartycka 18, 00-716 Warsaw, Poland*

arXiv:1401.3657v1 [astro-ph.GA] 15 Jan 2014

Accepted .... Received ...; in original form ...

ABSTRACT

Using a Monte Carlo code, we construct a dynamic evolutionary model of the Galactic globular cluster M22 (NGC6656). The initial conditions are chosen so that, after about 12Gyr of stellar and dynamical evolution, the model is an approximate fit to the surface brightness and velocity dispersion profiles of the cluster, to its mass function, and to the current binary fraction. Depending on the distribution of black hole natal kicks, we predict that the present-day population of stellar-mass black holes ranges from about 40 (no kicks) down to essentially zero (kicks distributed like those of neutron stars). Provided that natal kicks do not eject all new black holes, it is suggested that clusters with a present-day half-mass relaxation time above about 1Gyr are the ones that may still retain an appreciable population of black holes.

Key words: stellar dynamics – methods: numerical – globular clusters: individual: NGC6656

1 INTRODUCTION

For a long time, discussion of the role of black holes in globular clusters has been dominated by the theme of intermediate-mass black holes. While no-one would doubt that stellar-mass black holes once existed in these objects, one reason for their neglect is a long-standing theoretical prediction (Kulkarni, Hut, & McMillan 1993; Sigurdsson & Hernquist 1993) that there should be virtually none at the present day. As we shall see, this view is in need of revision, but in the meantime interest in the population of stellar-mass black holes in globular clusters was sustained by two ideas. The first is the realisation that they may be a prolific source of black-hole binaries and thus of sources of gravitational radiation (Portegies Zwart & McMillan 2000; Benacquista 2006; Belczynski et al. 2006; Moody & Sigurdsson 2009; Banerjee, Baumgardt, & Kroupa 2010; Downing et al. 2011; Tanikawa 2013). The second is the role that stellar-mass black holes play in the evolution of cluster cores (Merritt et al. 2004; Hurley 2007; Mackey et al. 2008).

This paper focuses on the black hole population itself, and, in particular, how many are to be expected at the present day in one particular old globular cluster. Thanks to software advances over many years, it is now quite straightforward to perform simulations of star clusters and to study the evolution of the black hole population directly. What is still hard, however, is to do this with models which resemble globular star clusters. The most sophisticated direct N-body techniques have been applied to this problem (Aarseth 2012, and several previous references by other authors), but the restriction to systems which initially possessed only of order 10^5 stars vitiates their direct application to all except the least populous globular clusters. There are two solutions, one being to *scale* the results of N-body models, provided that this can be done in a way which preserves the time-scales of the main evolutionary processes at work; the paper by Sippel & Hurley (2013) is an example, very relevant to the scientific aims of the present paper, and we return to it in our discussion (Sec.4.2). The second solution is the use of Monte Carlo codes, which are not restricted to small values of N, though they are less free of assumptions and approximations, and require cross-validation with N-body results in the range of N where the two techniques overlap (Giersz, Heggie, & Hurley 2008; Giersz et al. 2013). A Monte Carlo code is the main tool adopted in the present paper, but an independent code has also been applied to a similar problem by Morscher et al. (2013).

Even with a Monte Carlo code, however, different sets of initial conditions will give different answers for the number of stellar-mass black holes expected to survive to the present day. In previous papers (Heggie & Giersz 2008; Giersz & Heggie 2009, 2011) Monte Carlo evolutionary models for three clusters are described: M4, NGC6397 and 47 Tuc. The number of black holes throughout the evolution, which was not discussed much in these papers, is plotted in Fig.1. In our model of M4, no natal kicks were applied to black holes, but the population had decreased from about 1000 to one by an age of about 9Gyr (see Heggie & Giersz (2008, Fig.15)), and the last black hole escaped before 12Gyr. The last black holes were expelled from our model of NGC6397 even earlier. The contrast with our model of 47 Tuc is striking. Though natal kicks (with a 1-dimensional dispersion of 190km/s) were applied, and the num-

⋆ E-mail: d.c.heggie@ed.ac.uk (DCH); mig@camk.edu.pl (MG)

© 2002 RAS

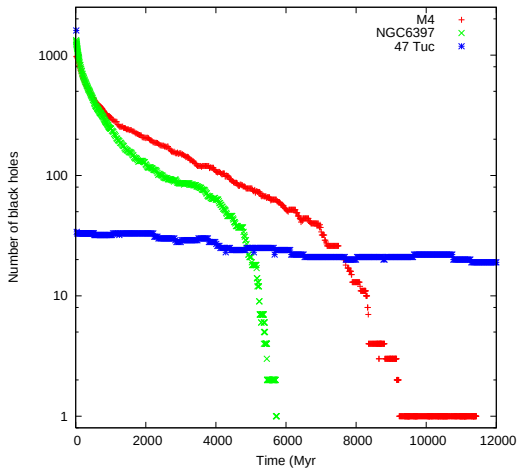

Figure 1. Number of stellar-mass black holes in published Monte Carlo models of three globular clusters. For the model of 47 Tuc, where natal kicks were applied, the results drop abruptly from the number initially created (about 1600).

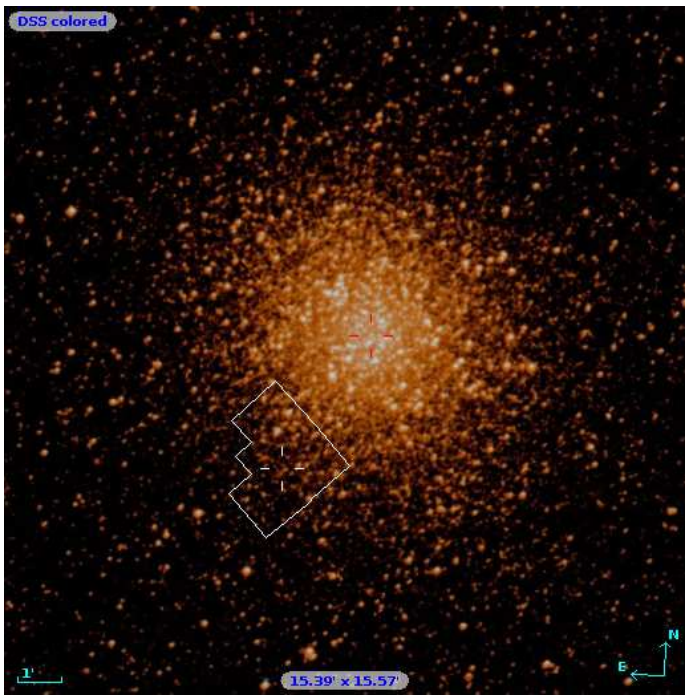

Figure 2. The field where the luminosity function of Piotto & Zoccali (1999) was obtained, overlaid on an optical image of M22. The luminosity function was obtained from only part of the WFPC2 field illustrated.

ber of retained black holes decreased abruptly to 34 (near the left margin of Fig.1), more than half were still present at 12Gyr.

The three examples in Fig.1 already raise an interesting question: how is it that our model of NGC6397, which initially retains far more stellar-mass black holes than 47 Tuc, ends up at the present day with none, while our model of 47 Tuc still has an appreciable population? The answer is that it depends on the phase of dynamical evolution in which the cluster is found. Our model of NGC6397 undergoes a phase of core collapse which ends at about the time when the last stellar-mass black hole escapes (Giersz & Heggie 2009), but for our model of 47 Tuc this phase of core collapse lies far in the future (Giersz & Heggie 2011). We return to this issue in Section 4.2, remarking here only that we refer to this episode as *second core collapse*, to distinguish it from a very early phase in which the mass segregation of the system of black holes comes to an end.

With reference to Fig.1, our aim in this paper is to provide similar theoretically-based expectations for the globular cluster M22 (NGC6656), motivated by the recent discovery in that cluster of two stellar-mass black holes (Strader et al. 2012), which may even represent only a sample of a considerably larger population. From what has been said, our first step will be to construct a Monte Carlo evolutionary model which, like those of the other three clusters we have studied, resembles the star cluster at the present day. This we do in the following section by iterating on the initial conditions so that, after 12 Gyr of evolution, the model provides an approximate fit to the observed surface brightness and velocity dispersion profiles of the cluster, and to its local stellar mass function (or, strictly, luminosity function). We repeat the exercise for different assumptions about the natal kicks of stellar-mass black holes, in each case reporting the number which survive to 12 Gyr (Sec.3). Our final section summarises our conclusions, and discusses them in the context of other recent research.

2 A MONTE CARLO MODEL OF M22

2.1 Observational data

Our source for the surface brightness profile of M22 is the compilation of Trager et al. (1995). As will be seen in Fig.5, the data are quite scattered (by about half a magnitude) within the core, and (surprisingly) a little fainter inside the core than at the edge of the core.

For the velocity dispersion profile we have adopted results from Lane et al. (2009, their Fig.3). The cluster rotates, with a maximum projected rotation velocity of about 3km/s (Lane et al. 2009, their Fig.2). It is not clear whether this has been removed from their velocity dispersion profile. In any event the rotation is one dynamical property of the cluster which cannot be modelled with the existing Monte Carlo technique; this is confined to non-rotating and spherically symmetric systems.

The stellar luminosity function we have used is the V luminosity function at a projected radius of about 4.5 arcmin given by Piotto & Zoccali (1999). This paper gives the data for each magnitude bin as the number of stars per 'HST area'; since the luminosity functions have been obtained from a single WFPC2 chip (see Fig.2), we take this to be an area of 1.78 arcmin^2 (based on data in the online *HST Data Handbook for WFPC2*). As the core radius is about 1.33 arcmin (Harris 1996), it is possible that appreciable mass segregation is present within the observed field, but only one luminosity function is given. In principle, the Monte Carlo model should be mapped to the observed field, but we have simply compared the observed luminosity function with that in the Monte Carlo model at the radius of the centre of the field.

Most other data on M22 (distance, metallicity, extinction) have been taken from the on-line revision of December 2010 of the

Harris catalogue (Harris 1996). The only exception is the binary abundance, where we have adopted a value of around 0.05 from the detailed results of Milone et al. (2012). Those results cover the region within the half-mass radius, and there is no statistically significant difference in the fraction inside the core. In fact changing the binary fraction within reasonable limits makes no appreciable difference to the overall evolution.

2.2 Model assumptions

The initial conditions we have adopted are similar (except of course for several numerical values, given in Secs.2.3 and 2.4) to those used in our previous papers (see especially Giersz & Heggie (2011, Table 1)). Briefly these are King models, with no initial mass segregation. The single stars have a two-part power law initial mass function in the range from 0.1 to $100M_{\odot}$, while the initial properties of the binaries are taken from Kroupa (1995). The Galactic tide is implemented as described in Giersz et al. (2013), but in any implementation it has to be treated as static in the Monte Carlo model. Note that Dinescu, Girard, & van Altena (1999) give for M22 an orbit with apo- and peri-galactic distances of about $R_a = 9.3$ and $R_p = 2.9$kpc, respectively, corresponding to an eccentricity (defined as $e = (R_a - R_p)/(R_a + R_p)$) of $e \simeq 0.52$. There is, however, substantial evidence from N-body simulations that a cluster on such an orbit retains a remarkably steady profile throughout each orbit (Küpper et al. 2010), and loses mass at a rate like a cluster on a circular orbit at a fixed intermediate radius (Baumgardt & Makino 2003). For the age of the cluster we have adopted 12Gyr, though it could be even older (Marín-Franch et al. 2009); and for the metallicity we have taken $Z = 0.0004$ (Harris 1996). Newly born neutron stars are given a kick using a Gaussian distribution with a one-dimensional dispersion of 190km/s, except for one model (Model C) reported in Sec.2.4 and subsequent sections of the paper, for which the dispersion was 253km/s. Natal kicks for black holes are more uncertain, and different choices are discussed (in connection with three models, called A,B,C), in Sec.3.1.

2.3 Initial parameter values

The procedure now is to choose parameters specifying the initial conditions (see Table 1) so as to optimise the fit of an evolved Monte Carlo model (Sec.2.2) to the observational data (Sec.2.1). In our previous papers, this has been a prolonged and laborious search, a process of trial and error guided by intuition. Since then it has been substantially automated. Our procedure now is to use the results of scaled models, i.e. Monte Carlo models with a number of stars N_* much smaller than the number of stars in the star cluster, but adjusted so that the relaxation time of the scaled model is the same as that of the actual cluster (see Heggie & Giersz (2008, Sec.2.4)). Then a measure of goodness of fit is constructed along χ^2 lines; for each kind of data (surface brightness, velocity dispersion and luminosity function) we adopt a single measure of the dispersion of the error, one for each kind of data, and based on information in the sources quoted in Sec.2.1. These are normalised by the number of data points in each kind of data, and simply summed, giving a measure Z of goodness of fit. (The Monte Carlo data are also subject to sampling error, but this has been ignored in the construction of Z.) Given values of the seven adjustable parameters in Table 1 (i.e. $N, r_t, r_h, W_0, \alpha_1, \alpha_2, m_b$), we run the Monte Carlo code and compute Z. To optimise over the parameter space we employ the Downhill Simplex algorithm, coded as *amoeba* in Press et al. (1992). For purposes of brevity in this paper we refer to this procedure as *ICFind*.

It is remarkable that the method is successful, as the algorithm is designed for optimisation of a smooth function, whereas the results of the Monte Carlo code are stochastic. Nevertheless it appears to converge, from a wide variety of starting points, after computation of order 50-100 models. For $N_* = 10^5$ this takes a few days. By "convergence" here we mean that the code finds a best model which cannot be improved on in the number of iterations stated; from other starting points, the best model may well be different. Unfortunately, even with this automatic method, we do not have any quantitative way of deciding the range of acceptable models, which would require improvement of our procedure for defining and calculating Z, and much greater computational effort. Furthermore, while computing the last 50 or so models, our experience is that the code evolves models with very similar initial conditions and chooses the best; it is, in effect, sampling the distribution of models which all result from these initial conditions by different choices of random numbers.

Results for 100% expulsion of black holes by natal kicks, and for 100% retention, are given in columns 2 and 3 of Table 1, referred to as Models a and c, respectively. From what has been said, it is not known whether the differences between these initial conditions are significant. Nevertheless it can be argued that the cluster will expand less with 100% expulsion (Merritt et al. 2004; Mackey et al. 2008), and therefore the larger value for the initial half-mass radius r_h in this case is what would be expected. Figs. 3 and 4 give an impression of the convergence of the run with 100% retention. We defer to the following subsection a discussion of how well the models agree with the observational data, as the full-sized models discussed in the next section are the focus of subsequent examination of the black hole population and its evolution.

The status of the listed retention factors requires some comment. We do not directly control this number, i.e. by ensuring that a given fraction of black holes are expelled. In our simulations, on the other hand, it is an indirect outcome of other choices, such as the dispersion of kicks (see Sec.3.1), as well as of the evolution of the model (which affects the escape velocity, for instance).

2.4 Full-sized models

The initial conditions in the second and third columns of Table 1 were determined with small-scale models, but results like these from *ICFind* have also been used as the basis of a number of full-scale models, i.e. models in which $N = N_*$. In some of these full-sized models the values given by *ICFind* were adjusted manually when it was judged that this might improve the fit with observations. For example the slope of the lower mass function might be altered when it was judged that this would further improve the fit with the luminosity function. Apart from N_*, the other main difference between the full-sized models and those from *ICFind* is that the runs have been carried out with a more advanced version of the Monte Carlo code, which is called MOCCA and is described in Giersz et al. (2013). The essential differences for the present purpose are (i) that escape of particles is modelled more closely on our current understanding of escape in tidal fields (rather than through the use of a tidal cut-off), and (ii) that three- and four-body interactions are calculated with a few-body code (*Fewbody*, see

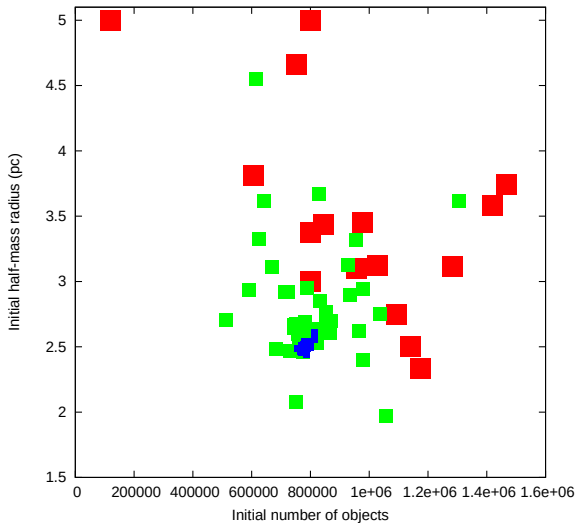

Figure 3. Convergence of the initial values of N and r_h, where N is the number of objects (single stars and binary stars) and r_h is the half-mass radius, for the determination of initial conditions in the case of 100% retention of black holes. The plot gives an impression of the range of values sampled by the code. Large symbols give the first 20 iterates, medium-sized symbols give iterates 21–60, and small symbols give the remainder (101 iterations altogether).

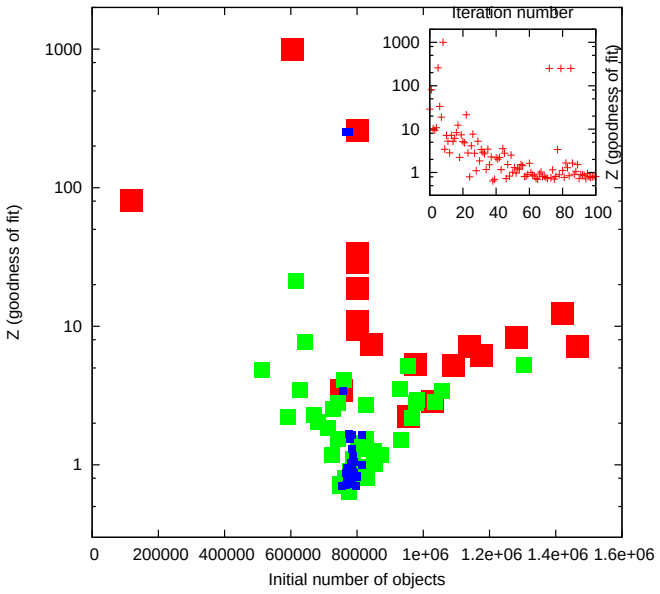

Figure 4. Marginal dependence of Z (a measure of goodness of fit) on the initial value of N (the initial number of objects), for the determination of initial conditions in the case of 100% retention of black holes. Default large values of Z may occur if the model failed to reach the required age of 12Gyr. Large values may also occur close to the best-fitting value of N (about 7.8×10^5) if other parameters are far from optimal. The meaning of the symbols is given in the caption to Fig.3. The inset gives the evolution of the goodness-of-fit parameter with iteration number.

Table 1. Initial conditions for M22, and the resulting black hole population

Model	a	c	A	B	C
$N_*/10^5$	1	1	9.21	8.32	7.57
$N/10^5$	8.0	7.8	8	8.32	7.57
r_t (pc)	93	100	77	89	102
r_h (pc)	3.1	2.5	2.67	2.72	2.43
W_0	3.7	2.9	6.0	7.4	2.93
α_1	1.1	0.90	1.12	1.21	0.90
α_2	2.7	2.7	2.43	2.72	2.8
m_b	0.73	0.67	0.84	0.96	0.67
N_{BH0}	–	–	1799	675	450
Retention factor	0%	100%	0.1%	62%	100%
N_{BH12}	–	–	2	14	43
N_{SBH12}	–	–	1	7	39
N_{BHBH12}	–	–	0	2	1
N_{BHNS12}	–	–	0	0	0
N_{BHWD12}	–	–	0	1	0
N_{BHMS12}	–	–	1	2	2

Explanation:

(i) N_* = the actual number of objects (single stars plus binary stars) in the model

(ii) N = the number of objects when the model is scaled to M22

(iii) r_t = initial tidal radius in parsecs

(iv) r_h = initial half-mass radius in parsecs

(v) W_0 = initial value of the scaled central potential of a King model

(vi) α_1, α_2, m_b: parameters of the initial mass function, which is a two-part power law with powers $m^{-\alpha}$, where $\alpha = \alpha_1$ for mass $m < m_b$, and $\alpha = \alpha_2$ above m_b.

(vii) N_{BH0} = number of stellar-mass black holes formed in the normal course of stellar evolution.

(viii) Retention fraction = fraction of black holes remaining after the escape of those escaping as a result of natal kicks.

(ix) N_{BH12} = number of stellar-mass black holes remaining at 12Gyr.

(x) $N_{SBH12}, N_{BHBH12}, N_{BHNS12}, N_{BHWD12}, N_{BHMS12}$ = number of single black holes, black hole-black hole binaries, black hole-neutron star binaries, black hole-white dwarf binaries, and black hole-main sequence star binaries, respectively, at 12Gyr.

Note: some other data on model B at 12Gyr are given in Sec.2.4.4.

Fregeau et al. 2004) instead of with cross sections. Since the mass-dependence of the cross sections used in the older code is based on theory, and the masses of black holes represent an extreme situation, it might be expected (because of the second of these changes) that the results could differ significantly from those of the older code.

So far we have computed almost 40 full-sized models, each of which takes a few days, though a few failed for technical reasons before reaching 12 Gyr (our assumed age for M22). The best of these, as judged by comparison with the observational data, use the initial conditions in the last three columns of Table 1, i.e. Models A, B and C. The basis of the initial conditions was a set of earlier runs of *ICFind* than those which produced Models a and c. Note that the values of N_* (the initial number of objects in the model) and N (the assumed initial number of objects in M22) are equal in Models B and C; in these full-scale runs we have generally not optimised over the choice of N, though Model A is an exception. For Model B, the quality of the fit to the observational data is displayed in Figs.5 – 7 and is discussed in detail in the following paragraphs, along with abbreviated comments about Models A and C.

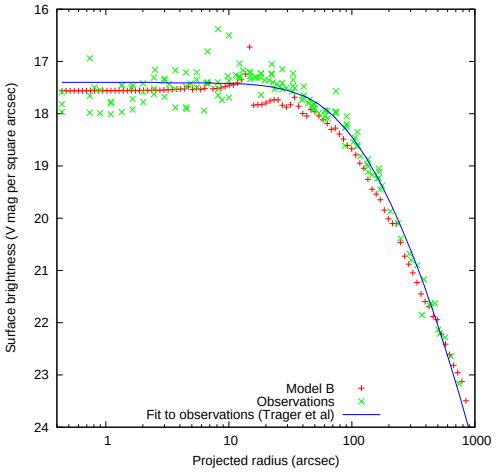

Figure 5. The surface brightness distribution of the Monte Carlo model (made with the new version of the code called MOCCA), with initial conditions in Column 5 of Table 1, compared with data from Trager et al. (1995). The solid line is their Chebyshev fit to the observation data. The result for the Monte Carlo model is obtained by treating each star as a spherical shell, and projecting the model on the sky. When a line of sight passes just inside the shell of a bright star the inferred surface brightness shows a spike, as in this model at a projected radius of about 15 arcsec.

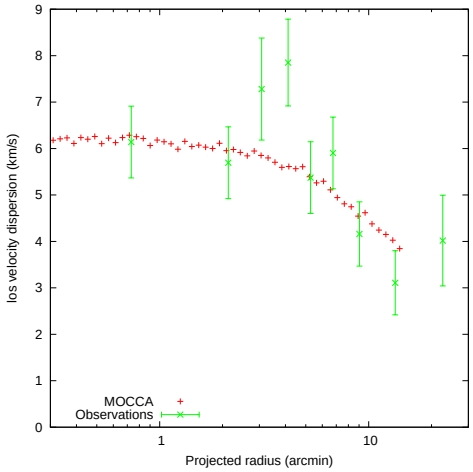

Figure 6. The line-of-sight velocity dispersion profile of the same model as in Fig.5, compared with data from Lane et al. (2009, their Fig.3). The model data are plotted only up to the outermost radius of the observational surface brightness profile shown in Fig.5.

2.4.1 Surface brightness profile

The surface brightness profile of the model is compared in Fig.5 with the observational data from Trager et al. (1995) and a Chebyshev polynomial fit which they provide. The model is generally somewhat fainter than the observations, by about 0.3 mag. It looks particularly faint at the edge of the core, especially when compared with the actual observational data and not to the smooth fit to the observational data. The mismatch looks considerably smaller in the halo, but the profile there is much steeper.

For Model A the surface brightness (not shown) is close to 17.5 up to a projected radius of 20 arcsec, too faint (by up to 0.5 mag in places) from there up to about 100 arcsec, and quite satisfactory thereafter. The surface brightness of Model C matches the observational data rather well (within the size of the symbols in Fig.5).

While this discussion has been expressed in terms of a comparison of surface brightness at a given radius, other interpretations are possible. For example, a model which exhibits an underluminous halo may simply be one that is too small (in radius).

2.4.2 The projected velocity dispersion profile

It is hard to characterise the fit of the velocity dispersion profile of Model B (Fig.6) with confidence, because of the large scatter in the observational data, but it may be best summarised by saying that it would be hard to improve. Perhaps the subjective impression is that the velocity dispersion of the model is a little too small, but a number of factors should be borne in mind. First, the outermost point includes stars close to the tidal radius (about 32 arcmin, according to Harris (1996)), where velocity dispersion profiles are elevated by the effects of the tidal field (Küpper et al. 2010)[1], and these effects are not included in the Monte Carlo models. Second, even with a binary fraction of 5%, the velocity dispersion may be elevated by the internal motion of binaries. Third, membership was determined on the basis of two spectral line indices, the radial velocity, and projected distance from the cluster centre, which led to the inclusion of only 345 stars out of the total of 3407 spectra, and so interlopers may still exist. Fourth, the typical uncertainty in the radial velocity of an individual star is about 3kms^{-1}. On the modelling side, it is also important to recall that the Monte Carlo model ignores the rotation of the cluster.

The projected velocity dispersion profile for Model A is very similar to that for Model B (just described), but for Model C the result is noticeably poorer. Though the central line-of-sight velocity dispersion is satisfactory at about 7 kms^{-1}, at larger radii it falls more steeply than the result for Model B shown in Fig.6, closely following the lower envelope of the observational data outside about 5 arcmin.

2.4.3 The local luminosity function

Compared with the observational data, the luminosity function of Model B (Fig.7) shows a deficit of stars brighter than turn-off ($m_V \simeq 18.4$) and in a section of the main sequence. At the brightest magnitudes the deficit may reach 0.5 dex or more, though the absence of error estimates in the observational data here makes this uncertain. In the rest of the main sequence the agreement seems satisfactory, especially in the absence of any estimate of the uncertainty in the Monte Carlo prediction. These results may go some way to explaining the fact that the surface brightness of the model is generally a bit too low (Sec.2.4.1).

[1] This is especially true around perigalacticon. Note that the current Galactocentric distance of M22 is 4.9kpc (Harris 1996), i.e. about one third of the way from peri- to apogalacticon.

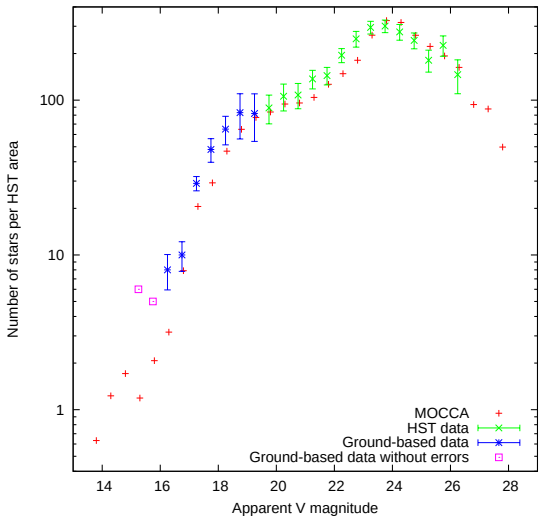

Figure 7. The luminosity function of the same model as in Fig.5, compared with data from Piotto & Zoccali (1999). Though some of this is ground-based, all the data is scaled to their HST field. The error bars, where available, have been read from their Figs.9 and 11.

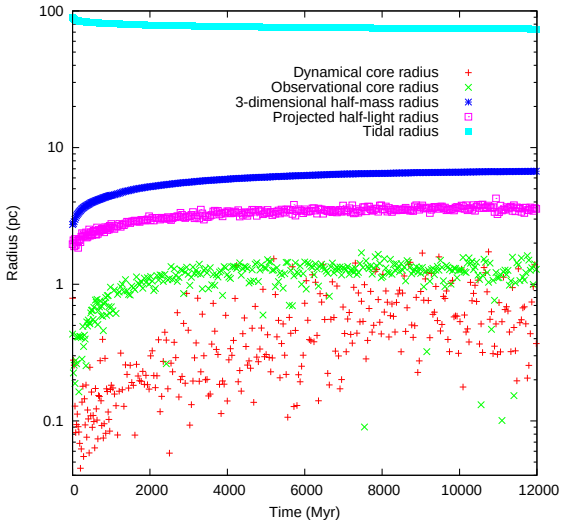

Figure 8. The evolution of the tidal radius, two versions of the half-mass radius, and two versions of the core radius, for Model B.

Since the agreement near turn-off seems satisfactory, it is difficult to understand how the deficit can rise so much within the small mass-range of stars brighter than turn-off, unless there is some flaw in the stellar evolution package in post-main sequence evolution. Similarly, it is difficult to know how the agreement along the main sequence could be improved by varying the mass function index α_1 (see Table 1).

The mismatch of the luminosity function of Model A to the observational data is of a similar magnitude to that for Model B, but is qualitatively different. The model has an excess of stars brighter than about magnitude 25, and a deficit at fainter magnitudes. Model C is qualitatively similar to Model B, except that the fit to the observational data is slightly worse around magnitude $m_V \simeq 18$ and around $m_V = 25$, but fits better between these limits.

2.4.4 Dynamical evolution

As we shall see in Sec.4, the dynamical evolutionary phase of a cluster is one of the main factors in assessing its likely population of stellar-mass black holes, and so we discuss the dynamical evolution of Model B here.

The initial mass of the model is about $5.70 \times 10^5 M_\odot$, and shrinks to about $3.20 \times 10^5 M_\odot$ at 12 Gyr. The resulting modest decrease in the tidal radius is shown in Fig.8. The value at the present day, about 73.6pc, greatly exceeds the observational value (Harris 1996) of about 29.7pc, but these can mean very different things in the case of a model which underfills its tidal radius, as here: the initial edge radius of the King model is 25.0pc, compared with the initial tidal radius of 89pc (Table 1). The value of the tidal radius of Model B is consistent with the Galactic potential. As mentioned in Sec.2.2, the Galactic orbit of the cluster takes it between 3 and 9 kpc from the Galactic Centre (Dinescu, Girard, & van Altena 1999), and in a Galactic potential with a flat rotation curve at 220km/s the range of tidal radii is from about 50 to 105pc, which includes the value in the model, but not the observational one.

Fig.8 also shows two versions each of the core and half-mass radii, i.e. a theorist's version and an observer's one. The observer's values compare well with those given in Harris (1996), which are about 1.24pc and 3.12pc for the core and half-light radii, respectively.

3 THE POPULATION OF STELLAR-MASS BLACK HOLES

3.1 Evolution of total numbers

Finally we turn to the main motivation of our study, which is the number of stellar-mass black holes at 12Gyr. Depending on the slope of the upper mass function, the number of stellar-mass black holes formed is between about 200 and 900 as the slope of the upper mass function, α_2, is decreased from 3.0 to 2.6. The numbers for the three best full-sized models are given in Table 1 and are labelled as N_{BH0}, although of course it is not the initial number. Though the numbers vary widely, this is almost entirely explained by the variation in α_2.

The subsequent evolution of the number of black holes depends crucially on the primordial kicks given to all new black holes, as these three models illustrate. If all new black holes are given a kick with a 1-dimensional dispersion of 190kms^{-1} (as is commonly considered for neutron stars), almost all escape promptly, and very few are still present at 12 Gyr. This is illustrated in Fig.9 by the data for Model A, and the final number is listed as N_{BH12} in Table 1. For this particular quantity the result has not been scaled from N_* to N, since the scaling factor is nearly unity.

In the absence of natal kicks, exemplified by Model C in Table 1 and Fig.9, the fraction of all stellar-mass black holes surviving at 12 Gyr is about 10%. Similar values were obtained in the small-scale models produced by *ICFind*.

The other recipe for natal kicks of black holes that we tried is the fall-back procedure of Belczynski, Kalogera, & Bulik (2002), which applies no kick if a large amount of mass from the supernova envelope falls back onto the degenerate remnant. Model B is the best of the full-sized models in which this procedure was adopted, and the fraction of black holes remaining at 12Gyr was about 2%.

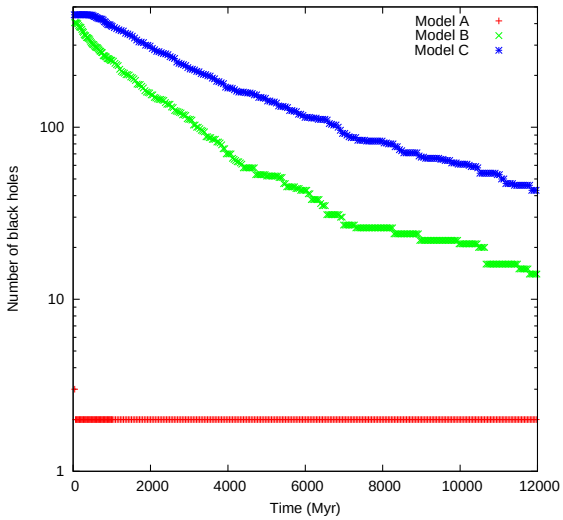

Figure 9. The evolution of the number of stellar-mass black holes in three models. For two models the initial number formed lies outside the plotted range, but is given in Table 1.

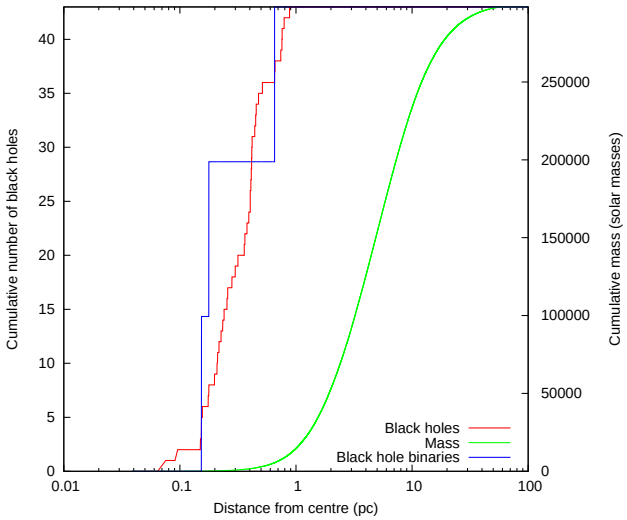

Figure 10. The spatial distribution of the black holes and black hole binaries in Model C at 12Gyr, compared with the spatial distribution of all stellar mass (including black holes). No axis labels or ticks are given for the number of black holes binaries (i.e. binaries in which at least one component is a black hole); the curve represents the cumulative fraction of the number, scaled to the vertical size of the frame. For comparison, the two black holes discovered by Strader et al. (2012) lie at *projected* radii of 0.25 and 0.4pc, respectively.

3.2 The black hole population at 12Gyr

As may be expected from the effects of mass segregation, the spatial distribution of the black holes at 12Gyr is very centrally concentrated (Fig.10, which shows data for Model C). The spatial distribution of the few binaries in which at least one component is a black hole is statistically indistinguishable. In addition to two-body interactions leading to mass segregation, such binaries are subject to energetic dynamical interactions which can send the binary into the halo of the cluster, but there is no evidence from Fig.10 that this is noticeable in their spatial distribution. In Model B the outermost black hole binary is at 0.35pc from the centre. The projected distances from the centre of M22 of the two black holes found by Strader et al. (2012) are 0.25pc and 0.4pc.

Table 1 gives more detail on the numbers of black hole binaries, broken down according to the type of the companion. Again as expected (from the effect of exchange interactions and their mass-dependence) the companions tend to be drawn from the relatively high-mass populations in the model. Because of the interest in finding a source for the emission of observed black holes in M22, details are given in Table 2 of the companions and orbital parameters. The binary identifier gives the model (Table 1) and the order in increasing radial distance within the model.

Unfortunately not one of these binaries is close to Roche-lobe overflow. Though the data correspond to conditions at a time close to 12Gyr, we have also checked that none of the black hole binaries are accreting at any time in the period 10–12Gyr, in any of the three full-sized models A–C. From the total of 59 black holes in these models, it follows that the probability that a black hole is accreting from a binary companion is at most a few percent. Therefore, if it is assumed that the two black holes in M22 have Roche-lobe filling companions, model A can be ruled out, i.e. the model in which all black holes experience natal kicks similar to those of neutron stars. This conclusion is model-dependent, however, for reasons given in the next paragraph and in Sec.4.3.

Despite the evidence of models A–C, we also checked three other models with rather similar initial parameters, and found altogether four examples of black holes accreting from evolving stellar companions. According to the models, accretion continued for at least 0.5Gyr, and so the probability that a black hole is accreting from a binary companion could indeed be a few percent. It is, however, difficult to estimate this probability, especially as it is likely to depend on the choice of parameters for the primordial binary population, and we have not attempted to explore this.

4 CONCLUSIONS AND DISCUSSION

4.1 Conclusions

Motivated by the recent discovery of two stellar-mass black holes in the Galactic globular cluster M22, we have constructed dynamic evolutionary models of this object in order to assess the survival of its population of black holes to the present day. We find that the result depends heavily on the assumptions made about natal kicks applied to new stellar-mass black holes. For kicks with a one-dimensional dispersion of 190km/s, the number of stellar-mass black holes at the present day is no more than one or two (Model A in Table 1). If no kicks are applied, then the fraction remaining at the present day is of order 0.1, resulting in a number of order 40 (Model C). Model B represents an intermediate, but physically motivated assumption about natal kicks, and results in a present-day population numbering 14.

We computed the dynamical evolution of our models with a Monte Carlo method. This code, of which we used two versions, includes two-body relaxation, binaries and their dynamical interactions, escape in the Galactic tide, and procedures for the internal evolution of both single and binary stars. Using a new procedure, we have explored hundreds of sets of initial conditions so as to produce models which, after 12Gyr of simulated evolution, resemble M22 in their surface brightness profile, velocity dispersion profile and stellar luminosity function. Possible initial conditions obtained

Table 2. Black hole binaries in models of M22

Binary	A1	B1	B2	B3	B4	B5	C1	C2	C3
Primary mass ($M_\odot$)	10.0	12.6	10.0	11.0	10.0	8.8	14.6	9.0	3.5
Companion mass ($M_\odot$)	0.23	0.78	9.9	0.69	10.0	0.64	10.0	0.33	0.61
Companion type	MS	MS	BH	MS	BH	WD	BH	MS	MS
Companion radius ($R_\odot$)	0.24	1.02	–	0.70	–	0.012	–	0.31	0.57
Semi-major axis ($R_\odot$)	312	177	106	132	399	449	112	157	161
Eccentricity	0.52	0.62	0.28	0.44	0.99	0.38	0.84	0.46	0.80

by this procedure are summarised in Table 1, and Figs.5–7 compare one of the evolved models with the observational data.

4.2 Black holes and cluster evolution

It is useful to try to draw some general lessons about the surviving black hole populations in old globular clusters from the modelling of M22 described in this paper, and from similar models of a few other objects, summarised here in Fig.1. Some, like M4 and NGC6397, lose all, or almost all, of their black holes well before the present day, while others (47 Tuc and M22) retain an appreciable fraction (assuming, in the case of M22, that natal kicks are moderated in some way). These facts are related to the evolution of the core. As we have seen (Fig.8) the core of M22 shows no sign of collapsing yet. Even the very concentrated cluster 47 Tuc is no more than half-way to core collapse (Giersz & Heggie 2011). Of the four clusters which are under discussion, these are also the two with appreciable residual populations of black holes (provided that kicks do not eject almost all new black holes).

The link between black hole populations and the evolution of the core has been noticed before (Merritt et al. 2004), and is underpinned by a recent theoretical treatment by Breen & Heggie (2013). These results show that expansion of the core (and indeed of the half-mass radius) can be driven by dynamical interactions among the black holes, which inevitably lead to their escape. Eventually the population of black holes is insufficient to sustain the flow of energy by relaxation in the outer parts of the cluster, and then the core begins to contract. As a result of this, energy is increasingly generated by interactions between the remaining black holes and the stars of lower mass, and the rate of escape of black holes declines. This change can be seen in Fig.9 at about the time when the core radius reaches its largest values (Fig.8). This phase of core contraction ends at what Breen & Heggie (2013) call "second core collapse" (the first being the original collapse of the black hole subsystem), when some other mechanism of generating energy (e.g. primordial binaries) becomes efficient enough.

The evolution of our model of M22 is more complicated than that of the idealised models considered by Breen & Heggie (2013), but does not differ qualitatively. Indeed, though stellar evolution also contributes to the early expansion of the half-mass radius, Giersz & Heggie (2011) showed that primordial binaries make little difference at the early stages (in their Monte Carlo model of 47 Tuc).

The upshot of these discussions is that appreciable populations of stellar-mass black holes are only to be expected in clusters which have not yet passed (second) core collapse. Other things being equal, this means clusters which have a sufficiently long evolutionary time scale, and we note that the half-mass relaxation times of NGC6397 and M4 are under 1Gyr ($\log t_{rh} = 8.60, 8.93$, respectively, according to Harris (1996)), while those of M22 and 47 Tuc exceed 1Gyr ($\log t_{rh} = 9.23, 9.55$, respectively).

These considerations allow us to synthesise not only our modelling of the four globular clusters that we have discussed, but also two other recent studies.

(i) Morscher et al. (2013) also used a Monte Carlo code to study the problem, though the model was not specifically geared to M22. The retention factor was high, about 86%, and more than half of the retained black holes still survived in the cluster at 12Gyr. We estimate the half-mass relaxation time at 12Gyr to be about 6×10^9yr, though this is based on the half-mass radius, whereas the estimates above are based on the half-light radii. Estimating these radii from Model B (Fig.8), we find that the comparable value of the half-mass relaxation time is about 2×10^9yr, a little larger than the value for M22.

(ii) The other model which we mention here is a direct N-body model (Sippel & Hurley 2013) with $N = 2.5 \times 10^5$ initially, and a similar binary fraction to our Monte Carlo models. Though smaller than M22 in mass, the larger initial radius of the N-body model gives it a value for the relaxation time at 12Gyr of about 2.1Gyr. The initial retention fraction was 10%, but even so 16 remained at 12Gyr. Naively, this would scale to about 50 for an initial model comparable in size to our suggested initial conditions for M22.

Despite this tidy picture, mention must be made of M62, which has a recently announced black hole candidate (Chomiuk et al. 2013), despite an uncomfortably low relaxation time: $\log t_{rh} = 8.98$.

4.3 Limitations of the modelling

Now we consider some aspects of the models which could have a bearing on these conclusions. In the first place we can make no claim for the uniqueness of the initial conditions we have derived. In particular, if more compact initial conditions exist (i.e. with a smaller half-mass radius), then the central escape velocity would be higher than in the existing models (for example, about 57km/s at the start of Model B), and the retention fraction of black holes would be greater, under any reasonable hypothesis on the magnitude of natal kicks.

More problematic are aspects of the evolutionary history of globular clusters which are not modelled at present in the Monte Carlo code. It has recently been suggested (Leigh et al. 2013) that accretion of interstellar gas (slow ejecta from stellar evolution) will act as a resistive force on the motions of black holes. This takes us to perhaps the most popular scenario for the formation of second generations in Galactic globular clusters (see, for example, D'Ercole et al. 2008), in which the ejected gas sinks to the centre of the original cluster of first-generation stars, and forms a second generation, while much of the first generation escapes. No evolutionary simulation yet includes these complex processes, and one can only argue qualitatively about how this may affect our conclusions.

In this scenario it is often argued that the first generation may be more massive than the second. Therefore the cluster in which the first generation of stellar-mass black holes formed would have had a much higher escape velocity than we have envisaged, making retention of a large fraction of these black holes much more likely. They would be centrally concentrated (by mass segregation), and would not be expected to escape, unlike much of the rest of the first generation. Equally, it is hard to see how the survival of black holes in the second generation would be adversely affected by being immersed in the potential well of the remaining first generation. Finally, these considerations suggest that sufficient numbers of black holes might well survive to the present day in this scenario, even if they were subject to natal kicks as in our model A.

ACKNOWLEDGEMENTS

We thank Jay Strader for guidance on the choice of observational data on M22, and the referee for his comments, which have markedly improved our efforts. This work was partly supported by the Polish Ministry of Science and Higher Education through the grant N N203 38036, and by the National Science Centre through the grant DEC-2012/07/B/ST9/04412.

REFERENCES

Aarseth S. J., 2012, MNRAS, 422, 841
Banerjee S., Baumgardt H., Kroupa P., 2010, MNRAS, 402, 371
Baumgardt H., Makino J., 2003, MNRAS, 340, 227
Belczynski K., Kalogera V., Bulik T., 2002, ApJ, 572, 407
Belczynski K., Sadowski A., Rasio F. A., Bulik T., 2006, ApJ, 650, 303
Benacquista M. J., 2006, LRR, 9, 2
Breen P. G., Heggie D. C., 2013, MNRAS, 432, 2779
Chomiuk L., Strader J., Maccarone T. J., Miller-Jones J. C. A., Heinke C., Noyola E., Seth A. C., Ransom S., 2013, ApJ, 777, 69
D'Ercole A., Vesperini E., D'Antona F., McMillan S. L. W., Recchi S., 2008, MNRAS, 391, 825
Dinescu D. I., Girard T. M., van Altena W. F., 1999, AJ, 117, 1792
Downing J. M. B., Benacquista M. J., Giersz M., Spurzem R., 2011, MNRAS, 416, 133
Fregeau J. M., Cheung P., Portegies Zwart S. F., Rasio F. A., 2004, MNRAS, 352, 1
Giersz M., Heggie D. C., 2009, MNRAS, 395, 1173
Giersz M., Heggie D. C., 2011, MNRAS, 410, 2698
Giersz M., Heggie D. C., Hurley J. R., 2008, MNRAS, 388, 429
Giersz M., Heggie D. C., Hurley J. R., Hypki A., 2013, MNRAS, 431, 2184
Harris W. E., 1996, AJ, 112, 1487
Heggie D. C., Giersz M., 2008, MNRAS, 389, 1858
Hurley J. R., 2007, MNRAS, 379, 93
Kroupa P., 1995, MNRAS, 277, 1507
Küpper A. H. W., Kroupa P., Baumgardt H., Heggie D. C., 2010, MNRAS, 407, 2241
Kulkarni S. R., Hut P., McMillan S., 1993, Nature, 364, 421
Lane R. R., Kiss L. L., Lewis G. F., Ibata R. A., Siebert A., Bedding T. R., Székely P., 2009, MNRAS, 400, 917
Leigh N. W. C., Böker T., Maccarone T. J., Perets H. B., 2013, MNRAS, 429, 2997
Mackey A. D., Wilkinson M. I., Davies M. B., Gilmore G. F., 2008, MNRAS, 386, 65
Marín-Franch A., et al., 2009, ApJ, 694, 1498
Merritt D., Piatek S., Portegies Zwart S., Hemsendorf M., 2004, ApJ, 608, L25
Milone A. P., et al., 2012, A&A, 540, A16
Moody K., Sigurdsson S., 2009, ApJ, 690, 1370
Morscher M., Umbreit S., Farr W. M., Rasio F. A., 2013, ApJ, 763, L15
Piotto G., Zoccali M., 1999, A&A, 345, 485
Portegies Zwart S. F., McMillan S. L. W., 2000, ApJ, 528, L17
Press W. H., Teukolsky S. A., Vetterling W. T., Flannery B. P., 1992, Numerical Recipes in Fortran, 2e, Cambridge, Cambridge University Press
Sigurdsson S., Hernquist L., 1993, Nature, 364, 423
Sippel A. C., Hurley J. R., 2013, MNRAS, 430, L30
Strader J., Chomiuk L., Maccarone T. J., Miller-Jones J. C. A., Seth A. C., 2012, Nature, 490, 71
Tanikawa A., 2013, MNRAS, 435, 1358
Trager, S. C., King, I. R., & Djorgovski, S. 1995, AJ, 109, 218

This paper has been typeset from a TEX/ LATEX file prepared by the author.